Model and Observation of Dispatchable Region for Flexible Distribution Network

Jun Xiao[1], Guoqiang Zu[2, 1], Ying Wang[1], Xinsong Zhang[3], Xun Jiang[4]

1. *Key lab of Smart Grid of Education Ministry, Tianjin University, Tianjin 300072, China*
2. *State Grid Tianjin Electric Power Research Institute, Tianjin 300384, China.*
3. *Nantong University, Nantong, 226019, China.*
4. *School of Engineering, Cardiff University, Cardiff CF24 3AA, UK*
Correspondence author: Guoqiang Zu, Email: zuguoqiang_tju@163.com

Highlights

- Region method is first used for flexible distribution network (FDN).
- The model and the observation approach of dispatchable region of FDN are proposed.
- The topological characteristics of dispatchable region of FDN are investigated.
- FDN and traditional distribution network are compared in region characteristics.

Abstract

Soft open points (SOPs), defined as the power electronic devices installed to replace normally open points in distribution network, can improve the flexibility of power control and thus further enhance the reliability and economy of power grids. Flexible distribution network (FDN) is a system-level concept to describe the distribution network equipped with multiple SOPs. Region method is to describe the secure range of the system operating in a geometric view. This paper adopts the region method to observe FDN for the first time. Firstly, the model of dispatchable region of FDN is proposed. The constraints of region space are formulated, considering SOPs, power flow, thermal capacity and voltage profile. Secondly, a simulation-based observation approach is also proposed to obtain the region projections on 2D and 3D sub-space. To illustrate the approach clearly, 2 small cases are given preceding a 7-feeders IEEE RBTS case. The region projections of case grids are observed and their topological characteristics are compared with those of traditional distribution network (TDN). The results indicate that FDN has advantages over traditional distribution network in operation security. For example, the region projections of FDN on 2-dimensional sub-space are about 2~4 times larger than those of TDN with the same network topology. The dispatchable region can be further developed into a useful tool for the secure and high-efficient operation of FDN in the future.

Keywords

soft open points, flexible distribution network, dispatchable region, model, observation.

1. INTRODUCTION

1.1 Motivation

ADVANCED power electronic technology is playing an increasingly important role in distribution network [1]. Soft open points (SOPs) refer to the flexible switches in distribution networks usually using back-to-back voltage source converters. SOPs are installed at a previously normally open points (NOPs) of distribution network [2]. SOP is able to provide the dynamic and continuous active/reactive power flow controllability and limit the short current [2]. Some pilot projects have demonstrated that SOP is beneficial to distribution network in many aspects, such as optimal power flow, load balancing, voltage regulation, power supply restoration, accommodation of distributed generation (DG), and so forth, which indicates its potential in the future distribution network [3][4]. In [5], a system-level concept, flexible distribution network (FDN), was proposed. FDN is defined as the distribution network with flexible power flow controllability using multi-terminal SOPs (including two-terminal SOPs). This concept is applied in this paper.

Security is the main objective of FDN operation. In a distribution system, the security requires that the system should maintain reliable power supply within thermal capacity and voltage profile limits under both normal operation state and single contingency. Paper [6] and [7] proposed a SOP-based method to mitigate the unbalanced condition of feeder load and remove overloading. Paper [8] proposed the voltage-VAR coordinated method based on SOP to eliminate the voltage violations. Paper [9] proposed a combined decentralized and local voltage control strategy based on SOP. In [10], a SOP-

based supply restoration model of FDN is established then solved by primal-dual interior-point algorithm. Paper [11] proposes a multiple-objective optimization framework of FDN. In terms of DG accommodation, paper [12] proposes a robust optimization method to achieve the robust optimal operation of SOPs in active distribution network. Paper [13] studies an adaptive service restoration strategy of distribution networks with distributed energy resources and SOPs.

The researches above make great progress in optimization models solution algorithm and simulation approach. However, in these researches, only single operation status of FDN is considered in single simulation process. Hence, different operation status cannot be linked up to obtain the integrated security status of FDN. Besides, the computing time is still too long for online real-time monitoring and dispatching due to the constantly varying operation status of FDN, although the algorithm performance has been improved a lot. For example, it takes about 60 seconds [8] to analyze an operation status on the IEEE 33-nodes test system.

1.2 Literature Review

Security region is defined as the set of all the secure operating points in the state space. Compared with the "point-wise" methods simulating or optimizing specific status, the region-based method has many advantages [14][15]. Firstly, the region can give the global information about the security. It can be calculated offline and applied online to judge whether an operating point lies inside the region. Moreover, we may know the relative location of the operating point, that is, the security margin to each boundary. Therefore, the time-series analysis can be rapidly performed by analyzing the motion path of the operating point. Finally, the boundary can be described by several hyperplanes approximately. Since FDN may contain plenty of uncertainties caused by large scale of intermitted DGs, this will help the probabilistic security assessment of FDN. Also, the region method can be used in the optimization and planning of distribution network.

The concept of distribution system security region (DSSR) was first proposed in [16]. Afterwards, the model [17], algorithm [18], topological characteristics [19] and implementation [20]-[22] of DSSR were step-by-step studied for the traditional distribution networks without SOPs. Existing researches have shown that the region-based method is effective for the security operation of distribution network. Paper [23] proposed the dispatchable region of power system for the first time, which is also essentially a special security region. However, it is focused on the security limits under normal operation state only and it is usually applied in operation optimization, such as network loss reduction and load balancing. In contrast, a security region is formulated towards contingency scenarios, where the power supply restoration is prioritized. Paper [24] and [25] proposed the model of dispatchable region of distribution network considering DGs and micro-grids. Paper [26] proposed a operational region of SOP, however, this region is device-level, cannot be used in the system-level dispatching of FDN. To sum up, the dispatchable region of FDN with SOPs are never studied.

1.3 Contributions

This paper proposes the dispatchable region of flexible distribution network (FDN-DR) for the first time. The model of FDN-DR is formulated, considering the new operation constraints for SOPs. The simulation-based approach to observe FDN-DR is also proposed. The topological characteristics of FDN-DR are observed on different case grids and compared to that of traditional distribution network (TDN). The results indicate the advantages of FDN in security operation.

2. CONCEPT OF FDN

2.1 Definition

TDN is designed in closed loop and operated in open loop, which limits the power supply reliability due to the power interruptions caused by switch operations after contingencies.

FDN is defined as the smart distribution network in closed-loop operation with the capability of wide-area energy distribution and exchange in the network [5]. SOP is a key electronic device that FDN should be equipped with to realize its functions. The other key technologies of FDN are as follows.

1) Planning: FDN should be built based on the existing network infrastructure and integrated with the emerging DC distribution network;

2) Operation: FDN should fit the existing distribution automation system;

3) Protection and control: new protection strategies should be developed to meet the fault characteristics of FDN.

2.2 Network Configuration

Due to the large scale of existing distribution network, it is a wise strategy to upgrade TDN to FDN smoothly based on the existing network topology. SOPs need to be placed on several key nodes only to save the investment for its high costs at present.

Take the single-loop cable network as an example. The switching station operates in open loop with two incoming lines, which origin from different upstream power resources. Fig. 1 shows the progress of upgrading a single-loop cable network to FDN by replacing the switching station with a SOP. Therefore, the closed-loop flexible operation of the two connected feeders is realized. Other typical network configuration of FDN can be found in [5].

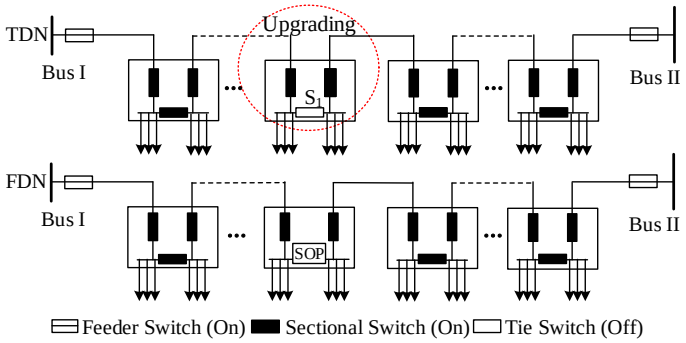

Fig. 1 The upgrade from a traditional single-loop cable network to FDN using a SOP

2.3 Features

The main features of FDN can be summarized as follows:

1) Closed-loop operation: FDN can block the short-circuit current at the close-loop point due to the isolation of DC link and instantaneous control of SOPs.

2) Flexibility and controllability: FDN can provide continuously, dynamic, fast active/ reactive power flow control among multiple branches in multiple directions.

3) Wide-area energy distribution and exchange: FDN can dispatch the power flow over the entire network through flexible networking devices. It can be regarded as the energy hubs, through which the power can be exchanged among feeders over an extensive power supply area.

3. Model of Dispatchable Region of FDN

The dispatchable region of FDN is defined as the set of all the operating points which satisfy the system normal operational constraints, mainly including the constraints of feeder capacity, substation transformer capacity and voltage profile, as well as the constraints of SOPs and DGs.

3.1 Operating Point

Considering the FDN with n non-slack nodes, the operating point is defined as an n-dimensional vector with net power of each node being the element. The operating point is formulated as (1)-(3).

$$\boldsymbol{W} = [S_1, ..., S_n] = [(P_1, Q_1), ..., (P_n, Q_n)] \tag{1}$$

$$P_i = P_i^L - P_i^G \tag{2}$$

$$Q_i = Q_i^L - Q_i^G \tag{3}$$

where $\boldsymbol{W}$ represents the operating point, S apparent power, P active power, Q reactive power. Subscript i denotes node i, L load and G DG. Let the direction be positive when the power flows out of node i. The net power of the node is limited due to the capacity constraints of devices connected to the node, such as distribution transformers and DGs, which are formulated as

$$|S_i| \leq C_i^{DT} \tag{4}$$

$$|S_i^G| \leq C_i^G \tag{5}$$

where C represents devices capacity. Superscript DT denotes distribution transformers. (4) represents the constraint of distribution transformers capacity. (5) represents the constraint of DG power output.

It should be noted that the power of SOPs is not included in the operating point. This is similar as the operating point of the security region of TDN [19][22], in which the status of the normal mechanical switches are also not included.

3.2 SOP Constraints

Considering a SOP with t interface terminals connected to t nodes of the distribution network, the operation of SOP should satisfy the constraints (6)-(8).

$$\sum_{i\in K}(P_i^{SOP}+\Delta P_i^{SOP})=0 \tag{6}$$

$$\Delta P_i^{SOP}=\alpha_i^{SOP}C_i^{SOP} \tag{7}$$

$$|S_i^{SOP}|=\sqrt{(P_i^{SOP})^2+(Q_i^{SOP})^2}\le C_i^{SOP} \tag{8}$$

where K is the set of t interface terminals of SOP. P_i^{SOP} represents the active power injecting into terminal i of SOP, Q_i^{SOP} reactive power, S_i^{SOP} apparent power. ΔP_i^{SOP} is the power loss at terminal i of SOP, α_i^{SOP} is factor of power loss. C_i^{SOP} is the capacity of terminal i. (6) is the equilibrium of active power from each terminal of SOP, including the power loss. (7) is power loss calculation of SOP. The operating efficiency of SOPs are usually over 98% thus can be reasonable ignored in some scenarios. (8) is the capacity constraint of SOP.

The operating state of SOPs can be also described by the vector $\boldsymbol{W}_{SOP}$, which includes the transmitted active power at t-1 independent terminals and reactive power at t terminals as elements. It is formulated as (9).

$$\boldsymbol{W}_{SOP}=[P_1^{SOP},...,P_{t-1}^{SOP},Q_1^{SOP},...,Q_t^{SOP}] \tag{9}$$

3.3 Power Flow Constraints

The power flow of branch and the voltage of each node can be calculated according to the operating point $\boldsymbol{W}$ and the operating state of SOP ($\boldsymbol{W}_{SOP}$). The DistFlow algorithm [27] is applied in this paper for its good performance in solving the power flow of distribution network. For $i, j\in V$, V is the set of connected buses. The power flow equations are formulated as (10)-(13).

$$\sum_{ji\in B}(P_{ji}-r_{ji}I_{ji}^2)+(P_i+P_i^{SOP})=\sum_{jk\in B}P_{ik} \tag{10}$$

$$\sum_{ji\in B}(Q_{ji}-x_{ji}I_{ji}^2)+(Q_i+Q_i^{SOP})=\sum_{jk\in B}Q_{ik} \tag{11}$$

$$U_i^2-U_j^2+(r_{ij}^2+x_{ij}^2)I_{ij}^2=2(r_{ij}P_{ij}+x_{ij}Q_{ij}) \tag{12}$$

$$I_{ij}^2U_i^2=P_{ij}^2+Q_{ij}^2=S_{ij}^2 \tag{13}$$

where B represents the set of all the branches of FDN, U_i the voltage amplitude of node i. Subscript ji represents the branch ji between node j and node i. r_{ij} and x_{ij} are the resistance and reactance of branch ji respectively. P_{ij} and Q_{ij} are the active power and reactive power transmitted through branch ji respectively and the positive direction is from i to j. Node i in (10)-(13) can be the slack node.

3.4 Security Constraints

The security constraints of FDN mainly include the feeder thermal capacity constraints, substation transformer capacity constraints and the node voltage constraints.

$$|S_{ij}|\le C_{ij} \tag{14}$$

$$S_i^T=\sum_{ij\in T_i}S_{ij}\le C_i^T \tag{15}$$

$$U_i^m\le U_i\le U_i^M \tag{16}$$

where C_{ij} represents the capacity of line ij. Superscript T represents the substation transformer. S_i^T represents the load power of substation transformer i, C_i^T the rated capacity. T_i is the set of all the branches from substation transformer i. U_i^m and U_i^M are the lower and upper voltage limit of node i. (14) is the constraint of line capacity. (15) is the constraint of substation transformer capacity. (16) is the constraint of node voltage. U_i^m and U_i^M are usually set as 0.93 and 1.07 for normal load nodes [30]. For DG nodes, U_i^m and U_i^M are usually set as 0.95 and 1.05.

3.5 Model

$$
\begin{aligned}
&\Omega_{FDR}=\{\boldsymbol{W}=[S_1,...,S_n]=[(P_1,Q_1),...,(P_n,Q_n)]\mid\\
&st.A\begin{cases}P_i=P_i^L-P_i^G\\ Q_i=Q_i^L-Q_i^G\\ \mid S_i\mid\le C_i^{DT}\\ \mid S_i^G\mid\le C_i^G\end{cases}\\
&st.B\begin{cases}\sum_{i\in K}(P_i^{SOP}+\Delta P_i^{SOP})=0\\ \Delta P_i^{SOP}=\alpha_i^{SOP}C_i^{SOP}\\ \mid S_i^{SOP}\mid=\sqrt{(P_i^{SOP})^2+(Q_i^{SOP})^2}\le C_i^{SOP}\end{cases}\\
&st.C\begin{cases}\sum_{ji\in B}(P_{ji}-r_{ji}I_{ji}^2)+(P_i+P_i^{SOP})=\sum_{jk\in B}P_{ik}\\ \sum_{ji\in B}(Q_{ji}-x_{ji}I_{ji}^2)+(Q_i+Q_i^{SOP})=\sum_{jk\in B}Q_{ik}\\ U_i^2-U_j^2+(r_{ij}^2+x_{ij}^2)I_{ij}^2=2(r_{ij}P_{ij}+x_{ij}Q_{ij})\\ I_{ij}^2U_i^2=P_{ij}^2+Q_{ij}^2=S_{ij}^2\end{cases}\\
&st.D\begin{cases}\mid S_{ij}\mid\le C_{ij}\\ S_i^T=\sum_{ij\in T_i}S_{ij}\le C_i^T\\ U_i^m\le U_i\le U_i^M\end{cases}\\
&\}
\end{aligned}
\tag{17}
$$

Based on the section 3.1-3.4 above, the dispatchable region of FDN can be formulated as the set of all $\boldsymbol{W}$ satisfying (2)-(16), which include the constraints of state space (*st. A*), SOP (*st. B*), power flow (*st. C*) and system security constraints (*st. D*). The compacted form of the dispatchable region of FDN model is shown in (17).

If an operating point $\boldsymbol{W}\in\Omega_{FDR}$ and makes any inequality of (17) just reaches the equal condition, it is said that $\boldsymbol{W}$ a boundary point of the dispatchable region of FDN.

4. OBSERVATION OF DISPATCHABLE REGION OF FDN

The dispatchable region of FDN is a closed hyper-geometry in the high-dimensional state space and is usually projected onto 2 or 3-dimensional sub-space to be observed. Based on the denseness of region [19], the simulation-based approach is proposed to obtain the 2 and 3-dimensional projections of region. The approach can be divided into 3 steps generally. Take the observation of 2-dimensional projections on sub-space (u, v) as an example. The flow chart of observation approach is shown in Fig.2.

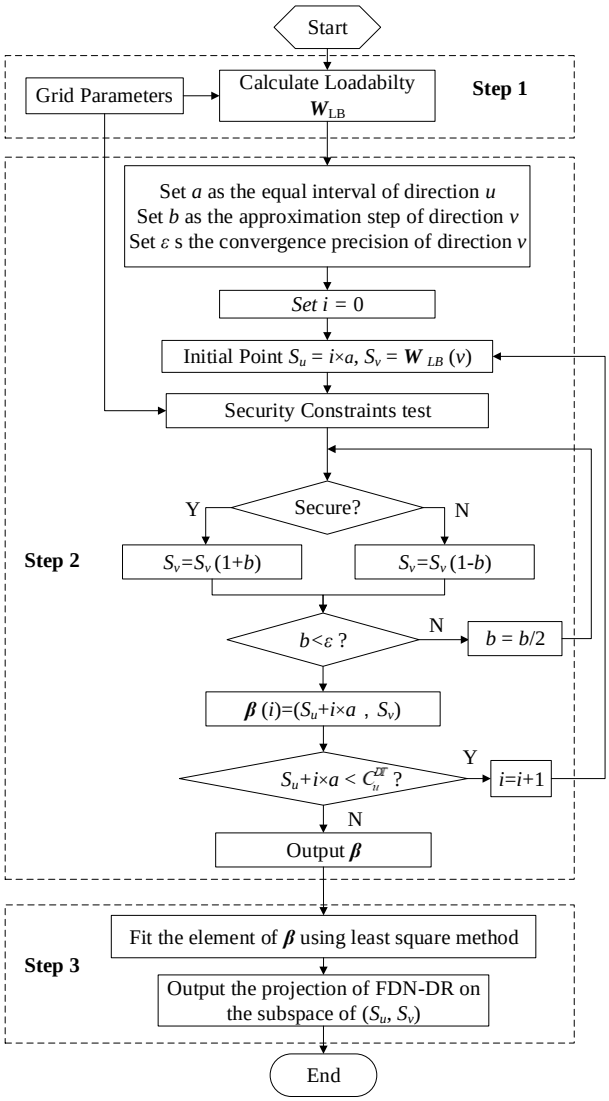

Fig.2 The flow chart of the proposed simulation-based observation approach of the dispatchable region of FDN.

Step 1 Calculate the initial point. The operating points closed to the region boundary are good candidates of the initial point for shortening the time of searching boundary points. Loadability is defined as the maximum power that a distribution network can supply within required normal operating constraints. The loadability can be calculated by the method in [28]. The loadability of TDN with the same network topology of FDN is used as the initial point. The step 1 includes:

1-1) Based on the network topology, calculate the loadability (denoted as LB) and the load distribution vector of loadability (denoted as $\boldsymbol{W}_{LB}$).

1-2) Choose the power of node u and v (denoted as S_u and S_v) as free variables and froze the power of other nodes at the corresponding elements of $\boldsymbol{W}_{LB}$.

1-3) The initial point in 2-dimensional sub-space is (0, $\boldsymbol{W}_{LB}(v)$), where $\boldsymbol{W}_{LB}(v)$ is the power of node v when the system reaches at loadability.

Step 2 Calculate the critical security point (boundary point) using simulation-based approach.

2-1) In the direction of u, generate a series of points between [0, C_u^{DT}] with the equal interval a. C_u^{DT} is the capacity of distribution transformer at node u.

2-2) Verify whether the initial point (S_u, S_v) satisfies the constraints of (17). $S_u = 0$, $S_v = \boldsymbol{W}_{LB}(v)$. The verification is performed on the simulation platform developed by MATLAB and OpenDSS.

2-3) Adjust S_v with the starting step size b. If the result of verification is "Yes", $S_v = S_v(1+b)$, otherwise, $S_v = S_v(1-b)$.

2-4) Let the convergent precision value be ε. Judge whether $b < \varepsilon$. If so, denote ($S_u + i \times a$, S_v) as the *ith* element of the vector $\boldsymbol{\beta}$. If not, let $b = b/2$ then repeat step 2-2) and 2-3) until $b < \varepsilon$.

2-5) Judge whether the point on direction u (S_u) is out of the state space. If $S_u + i \times a < C_u^{DT}$, let $i = i+1$ and generate a new

operating point to be verified then return to step 2-2). If $S_u+i\times a \geq C_u^{DT}$, the procedure is ended and the vector $\boldsymbol{\beta}$ is output.

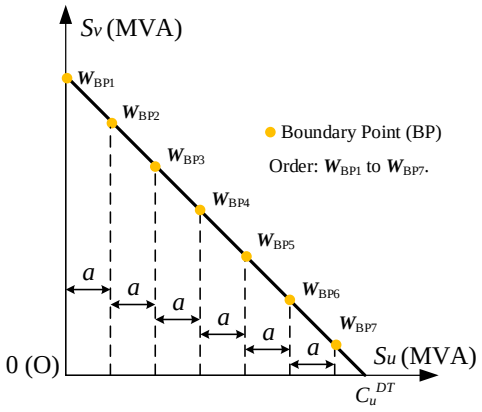

Fig.3 The generation of all boundary points. $\boldsymbol{W}_{BP1}$~$\boldsymbol{W}_{BP7}$ are one-by-one generated.

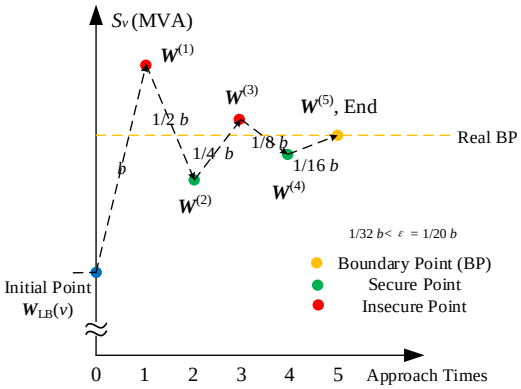

Fig.4 The searching process for a certain boundary point in the Fig.3.

A group of figures are used to further illustrate the **Step 2**. Fig.3 represents the solution order of boundary points. The Fig.4 shows the searching process to obtain each boundary point.

Step 3 According to the $\boldsymbol{\beta}$ which contains all the critical points, the least square method is used to fit all the critical points as a linear figure (straight line in 2-dimesional sub-space). The 2-dimensional boundary figure of (u, v) is obtained.

Using loadability is important to observe the dispatchable region projections of FDN because the security-related problem is significant in heavy load scenario. If the load ratio is low, the proposed observation approach is also compatible when the loadability is replaced by the zero point as the initial point.

5. Case Study

In this section, the dispatchable regions of FDN and TDN case grids with the same network topology are observed and compared. The similarities and differences between dispatchable region of FDN and TDN are summarized. Three case grids are studied in total, which are the single-loop network case, the 3-feeder connected case and the modified 7-feeder IEEE RBTS case.

5.1 Single-loop Network Case

The single-loop network case grids for both TDN and FDN are shown in Fig.5. The case parameters are shown in table I.

TABLE I
PARAMETERS OF SINGLE-LOOP NETWORK CASE

	Capacity (MVA)	Length (km)	Resistance (Ω/km)	Reactance (jΩ/km)
Line1,2,3	6.997	3	0.08	0.09
SOP	8		U_0=10.5 kV	

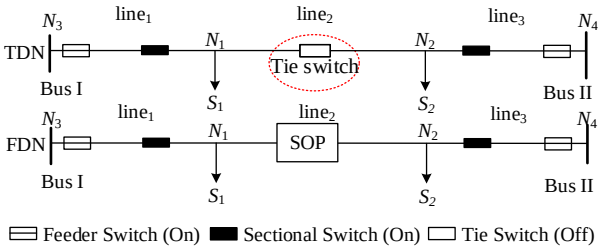

Fig. 5 Single-loop network case (overhead lines)

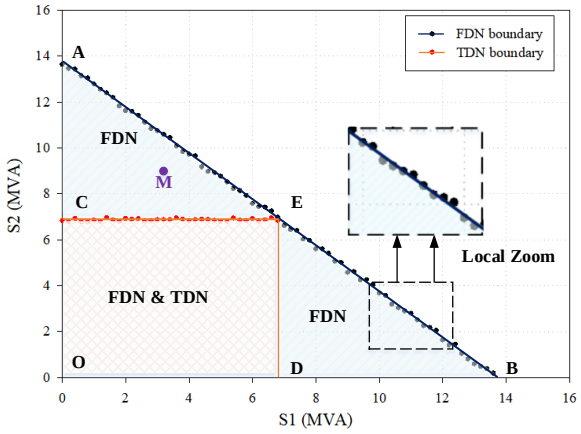

Fig. 6 Dispatchable region projections of TDN and FDN of single-loop network case. The local zoom of boundary of FDN is to show its approximate linear property.

The 2-dimensional projections of dispatchable regions of FDN and TDN are obtained and shown in Fig.6 using the observation approach proposed in section IV. The algorithm was developed in MATLAB with OpenDSS solving the power flow then run on a computer with Intel Core i3 CPU, 2.0 GHz, 4 GB RAM. The resolution time is 1.1s.

The 2-dimensional dispatchable regions of FDN and TDN are compared and the results are summarized as follows.

(1) The approximate triangle OAB is the dispatchable region projection of FDN and the approximate rectangle OCED is the dispatchable region projection of TDN. O is the original point of 2-dimensional sub-space. AB is the security boundary of FDN dispatchable region. CE and ED are the security boundaries of TDN dispatchable region. The security boundaries are corresponding to the limits of either the thermal capacity or voltage profiles. In this case, the security boundaries are all for feeder thermal capacity limits.

(2) The size of FDN dispatchable region projection (about 93.8 MVA^2) is about 2 times larger than TDN dispatchable region projection (about 46.9 MVA^2). This means that the secure operating range of FDN is about 2 times more than that of TDN for the same network topology in normal operating states. In other words, FDN is more secure than TDN with the same network topology. Take operating point M (3.5MVA, 9MVA) as an example ($\cos\varphi = 0.9$). For TDN, M is outside the region and is insecure because $line_3$ is overloading (9.098MVA > 6.997MVA (capacity of $line_3$), Table II). For FDN, however, M is inside the region and is secure because SOP can adjust the power flow according to certain optimal strategy to remove the overloading (6.571 MVA< 6.997MVA, Table II). The power flow data at M is show in table II.

TABLE II
THE POWER FLOW DATA AT OPERATING POINT M(3.5,9)

	TDN	FDN
S1 (MVA) $\cos\varphi = 0.9$	3.5	3.5
S2 (MVA) $\cos\varphi = 0.9$	9	9
Trans power-Line1 (MVA)	3.033	6.062
Power loss-Line1 (MVA)	0.033	0.062
Trans power-Line3 (MVA)	**9.098(overloading)**	**6.571**
Power loss-Line3 (MVA)	0.098	0.067
Trans power-SOP (from N2 to N1, MVA)	0	2.5
Power loss-SOP (MVA)	0	0.005
Total power loss	0.131	0.134
U1 (kV)	10.42	10.35
U2 (kV)	10.21	10.33

U3 (kV)	10.5	10.5
U4 (kV)	10.5	10.5

(3) The maximum load which can be supported by single feeder of FDN within security constrains is about 13.7 MVA (for example, S_1=0 MVA and S_2=13.7 MVA). This is a simple but interesting fact because the maximum load of single feeder should be definitely lower than the feeder capacity itself in TDN planning guidelines. However, this rule could be changed for FDN, that is, the single feeder of FDN might supply more load than the feeder capacity itself, because SOP can re-distribute the load from one feeder to the other connected feeders especially when the load curve is complementary among connected feeders.

(4) It can be seen that the region boundaries of TDN and FDN in Fig.6 are all highly approximate linear, which is consistent with the conclusion of the research on dispatchable region or security region before [23][24]. Therefore, the simplified figure is used in the following sections of this paper to illustrate the region characteristics more clearly. The simplified figure of Fig.6 is shown in Fig7.

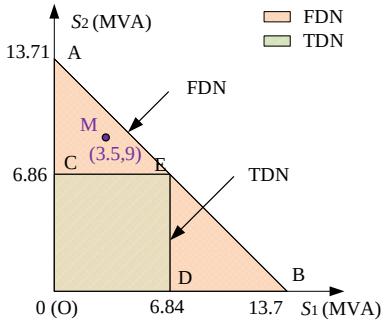

Fig. 7 Dispatchable region projections of FDN and TDN of single-loop network case (simplified).

5.2 Two-feeders Connected Network Case

The 3-feeder connected network case grid is original from the real FDN project, which is the world's first three-terminal SOP-based pilot project of medium-voltage FDN, located at Beijing, China [5]. The project schematic diagram is shown in Fig. 8. Centered with a three-terminal AC/DC hybrid SOP, two single-loops integrating loads and DGs are coupled to form a closed-loop distribution network. Two centralized PV power stations are connected to the 10 kV buses.

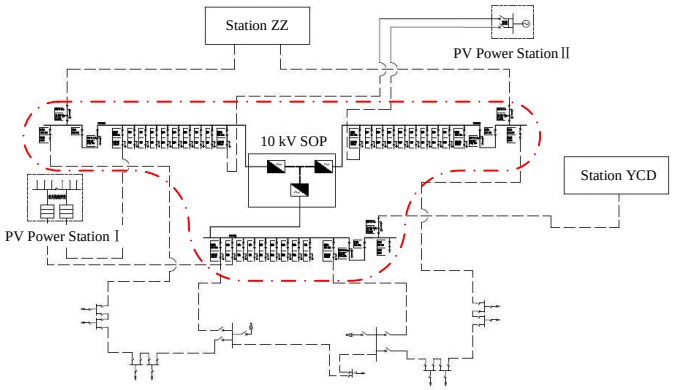

Fig.8 The diagram of the FDN pilot project

The brief network topology is shown in Fig.9. The feeders are connected in a switch station using SOP. To ensure the comparability, the 3-feeders case parameters are modified in consistent with the single-loop network case (Table I). The output power of PV power station Ⅰ and II is expected to be 1.7MW and 0.98MW. The 3-dimensional and 2-dimensional region projections are both observed, where S_1= S_{L1}-S_{G1}, S_2= S_{L2}-S_{G2}.

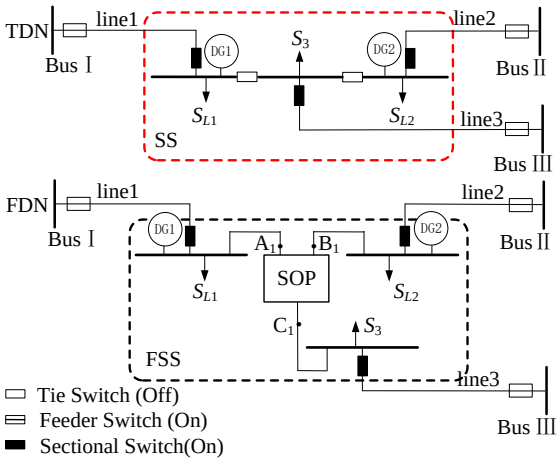

Fig.9 3-feeder case topology of TDN and FDN

5.2.1 Three-Dimensional Region

The 3-dimensional projections of both FDN dispatchable region and TDN dispatchable region are shown in Fig.10. Since the operating point vectors of 3-feeder case are just 3-dimensional, the 3-dimensional projection is also the total-dimensional [29] for this case.

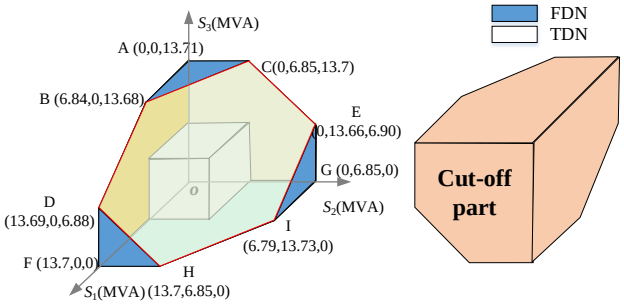

Fig. 10 3D dispatchable region projections of TDN and FDN of 3-feeder case

As is shown in Fig.10, the 3-dimensional FDN dispatchable region and TDN dispatchable region are both approximate closed polyhedrons surrounded by hyperplanes. FDN dispatchable region is the larger cube polyhedron, which can be obtained by cutting an approximate cube with the edge length of about 13.7 MVA. The cut-off part is shown in the right of Fig.10 and the remaining part (heptahedron) is the FDN dispatchable region. The shape of the cut-surface is hexagon (BDHIEC).

TDN dispatchable region is the approximate cube with the edge length of 6.85 MVA. The vertex outermost from the original point is just upon the cut-surface of FDN dispatchable region and thus the TDN dispatchable region is smaller than FDN dispatchable region and contained in the FDN dispatchable region.

5.2.2 Two-Dimensional Projections

The 2-dimensional projections of FDN dispatchable region and TDN dispatchable region are shown in Fig.11. The S_1 and S_2 are chosen as observation variables and S_3 is frozen at 2.7 MVA here.

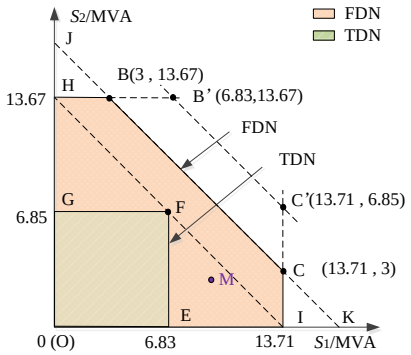

Fig. 11 2D dispatchable region projections of TDN and FDN of 3-feeder case

(1) As is shown in Fig.11, the FDN dispatchable region projection is the approximate pentagon (OHBCI) with the size of about 130.4 MVA^2. The TDN dispatchable region projection is the approximate rectangle (OGFE) with the size of about 46.9 MVA^2. The projection size of FDN dispatchable region is about 2.7 times larger than that of TDN dispatchable region.

(2) The size of FDN dispatchable region of 3-feeders case is about 1.4 times larger than that of single-loop network case in Fig.7. Particularly, if S_3 is frozen at 0 MVA, the boundary of FDN dispatchable region will be B'C' and the size will be about 1.75 times larger than that of single-loop network. This means that the secure operating range of multi-connected feeders can be improved to greater degree than single-loop network using SOP, because more feeders will supply the load together through SOPs and share the remaining feeder capacity.

The power flow data at operating point M in Fig.11. is shown in table III. M here is inside FDN dispatchable region but outside TDN dispatchable region.

TABLE III
THE POWER FLOW DATA AT OPERATING POINT M (9,3)

	TDN	FDN
S_1 (MVA) cosφ = 0.9	9.3	9.3
S_2 (MVA) cosφ = 0.9	3	3
S_3 (MVA) cosφ = 0.9	2.7	2.7
DG_1 (MVA)	1.7	1.7
DG_2 (MVA)	0.98	0.98
Trans power-Line1 (MVA)	**9.207(overloading)**	**4.975**
Power loss-Line1 (MVA)	0.093	0.025
Trans power-Line2 (MVA)	2.97	4.975
Power loss-Line2 (MVA)	0.03	0.025
Trans power-Line3 (MVA)	2.673	4.975
Power loss-Line3 (MVA)	0.027	0.025
Trans power-SOP (from A1 to B1, MVA)	0	2
Trans power-SOP (from A1 to C1, MVA)	0	2
Trans power-SOP (from B1 to C1, MVA)	0	0
Power loss-SOP (MVA)	0	0.004
Total power loss	0.15	0.079
U_{A1} (kV)	10.02	10.17
U_{B1} (kV)	10.21	10.19
U_{C1} (kV)	10.29	10.20

5.2.3 Modified 7-feeders IEEE RBTS case

In this section, the FDN dispatchable region of a practical case is demonstrated. The case grid is modified from IEEE RBTS Bus 4 test system[31], which is shown in Fig.12. All the nodes between the feeder outlet and tie switches are combined as one node to reduce the dimension of the operating points. Therefore, one feeder is corresponding to one node in this case. The case parameter is shown in table IV.

TABLE IV
PARAMETERS OF MODIFIED 7-FEEDERS IEEE RBTS CASE

	Capacity (MVA)	Length (km)	Resistance (Ω/km)	Reactance (jΩ/km)
F1-F3	8.92	4	0.07	0.08
F4-F7	8.92	5	0.07	0.08
T1-T6	10	/	/	/
SOP	9	/	/	/

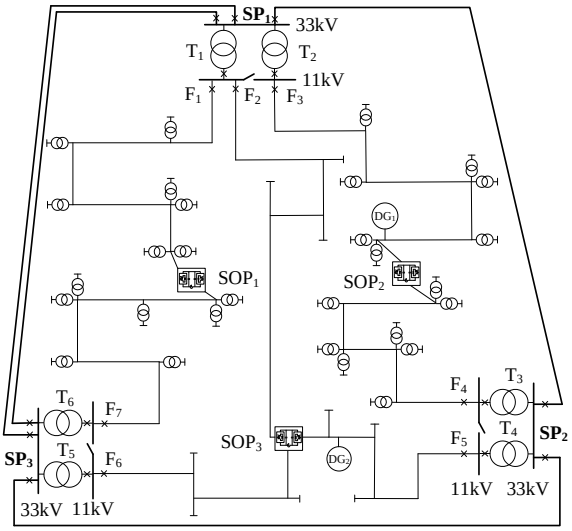

Fig. 12 FDN test system modified from IEEE RBTS Bus 4

The 2-dimensional FDN dispatchable region and TDN dispatchable region projections are observed. Different types of feeder pairs are chosen as observation variables. The other feeder loads are frozen at $\boldsymbol{W}$, where $\boldsymbol{W}$ = (3.011,3.011,4.96,4.942,4.578,3.978) (unit: MVA). This is the operating point under maximum load supply level of TDN with same network topology, which is also the heavy load scenario for FDN. The output power of DG_1 and DG_2 is expected to be 0.5 MVA and 0.6 MVA. The types of feeder pairs include the single-loop feeders (F1, F7), multi-connected feeders (F2, F6) and the feeders from the same substation transformers (F1, F2). The FDN dispatchable region and TDN dispatchable region 2-dimensional projections are shown in Fig.13 (a)-(c).

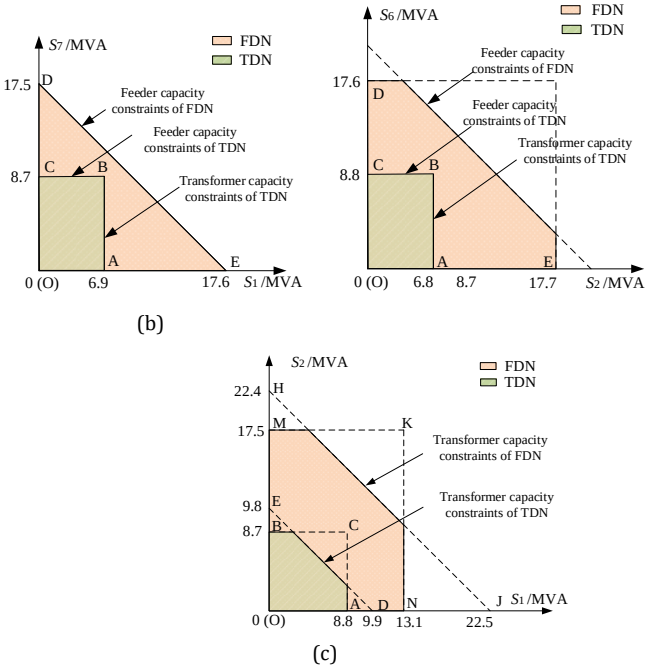

Fig. 13 (a) 2D dispatchable region projections of TDN and FDN of single-loop feeder pairs of 7-feeder IEEE RBTS case (F1, F7); (b) 2D T dispatchable region projections of TDN and FDN of multi-connected feeder pair of 7-feeder IEEE RBTS case (F2, F6); (c) 2D dispatchable region projections of TDN and FDN of feeder pair from the same substation transformer of 7-feeders IEEE RBTS case (F1, F2)

As is shown in Fig.13,

1) The size of FDN dispatchable region is obviously larger than that of TDN dispatchable region (respectively about 2.6 times, 3.6 times and 4 times), which is the same as the results of the single-loop network case and 3-feeder case. The difference is that the FDN dispatchable region and TDN dispatchable region here are constrained by not only the feeder capacity limit, but also the capacity limit of substation transformers.

2) The region projection of multi-connected feeder case (Fig.13-b) extends to pentagon with larger size compared with that of single-loop network case (Fig.7). The reason is that more than one feeder will together supply the load of the heavy or overloading feeder. This result is same as the 3-feeders case of section V.B.

3) The feeder of FDN is able to supply the load, which is larger than the capacity of the feeder itself. In all three figures, the feeder of FDN can supply about 17.6 MVA at most, which is larger than the feeder capacity (8.92MVA).

6. CONCLUSIONS

This paper adopts region method to observe the FDN for the first time. The model and observation approach of dispatchable region of FDN using SOPs are both proposed and tested on different case grids, which gives out an effective way to find the dispatchable region of FDN more easily. The dispatchable region of the FDN and TDN are compared. The results, for example, the larger region size, indicate that FDN has distinct advantages over TDN in security operation. The main conclusions and suggestions are as follows.

1) From the aspect of region size, the projection of FDN dispatchable region on 2-dimensional sub-space is about 2~4 times larger than that of TDN dispatchable region with the same network topology. The reason is that FDN can adjust the power flow flexibly to remove overloading and voltage violations.

2) The feeder of FDN can supply the load which is larger than the capacity of the feeder itself because the other connected feeders can help to share the load through SOPs. This is a breakthrough for the distribution network planning guideline and will provide new ideas to deal with the local load increase.

3) The upgrading of multi-connected feeders with SOPs can achieve better effect than single-loop network on the load ratio improvement. This is useful for the siting of SOPs.

This paper proposes a new idea for the high-efficient and secure operation of FDN based on region method. Future research will include the model of FDN dispatchable region considering N-1 reliability criterion and the DG accommodation in FDN.

ACKNOWLEDGEMENTS

The authors gratefully acknowledge the National Key Research and Development Program of China (2016YFB0900100) and National Natural Science Foundation of China (51877144).

REFERENCES

[1]. HEYDT, Gerald Thomas. The next generation of power distribution systems. IEEE Transactions on Smart Grid, 2010; 1(3): 225-235.

[2]. Cao, W., Wu, J., Jenkins, N., Wang, C., & Green, T. Benefits analysis of Soft Open Points for electrical distribution network operation. Applied Energy, 2016; 165: 36-47.

[3]. DISTRIBUTION, Western Power. Low Carbon Networks Fund submission from Western Power Distribution–Network Equilibrium. 2016. Available Online: https://www.ofgem.gov.uk/publications-and-updates/, 2016

[4]. SP Energy Networks, Electricity NIC submission: SP Energy Networks – ANGLE-DC Available Online: https://www.ofgem.gov.uk/publications-and-updates/electricity-nic-submission-sp-energy-networks-angle-dc, 2016

[5]. Xiao, J., Wang, Y., Luo, F., Bai, L., Gang, F., Huang, R.& Zhang, X. Flexible distribution network: definition, configuration, operation, and pilot project. IET Generation, Transmission & Distribution, 2018; 12(20): 4492-4498.

[6]. Cao, W., Wu, J., & Jenkins, N., "Feeder load balancing in MV distribution networks using soft normally-open points," 2014 *IEEE PES Innovative Smart Grid Technologies*, Europe, Istanbul, 2014, pp. 1-6.

[7]. Ji, H., Wang, C., Li, P., Zhao, J., Song, G., Ding, F., & Wu, J. An enhanced SOCP-based method for feeder load balancing using the multi-terminal soft open point in active distribution networks. Applied energy, 2017; 208: 986-995.

[8]. Li, P., Ji, H., Wang, C., Zhao, J., Song, G., Ding, F., & Wu, J. Coordinated control method of voltage and reactive power for active distribution networks based on soft open point. IEEE Transactions on Sustainable Energy, 2017; 8(4): 1430-1442.

[9]. Li, P., Ji, H., Yu, H., Zhao, J., Wang, C., Song, G., & Wu, J. Combined decentralized and local voltage control strategy of soft open points in active distribution networks. Applied energy, 2018;241, 613-624.

[10]. Li, P., Song, G., Ji, H., Zhao, J., Wang, C., & Wu, J., "A supply restoration method of distribution system based on Soft Open Point," 2016 *IEEE Innovative Smart Grid Technologies - Asia (ISGT-Asia)*, Melbourne, VIC, 2016, pp. 535-539.

[11]. Qi, Q., Wu, J., & Long, C. Multi-objective operation optimization of an electrical distribution network with soft open point. Applied energy, 2017; 208, 734-744.

[12]. Ji, H., Wang, C., Li, P., Ding, F., & Wu, J. Robust operation of soft open points in active distribution networks with high penetration of photovoltaic integration. IEEE Transactions on Sustainable Energy, 2018; 10(1), 280-289.

[13]. Lou, C., & Yang, J. "Adaptive Service Restoration Strategy of Distribution Networks with Distributed Energy Resources and Soft Open Points." (2019). CIRED, Madrid.

[14]. Ding, T., Bo, R., Sun, H., Li, F., & Guo, Q. A robust two-level coordinated static voltage security region for centrally integrated wind farms. IEEE Transactions on Smart Grid, 2015; 7(1), 460-470.

[15]. Chen, S., Wei, Z., Sun, G., Wei, W., & Wang, D. Convex Hull Based Robust Security Region for Electricity-Gas Integrated Energy Systems. IEEE Transactions on Power Systems, 2018; 34(3), 1740-1748.

[16]. Xiao, J., Gu, W., Wang, C., & Li, F. Distribution system security region: definition, model and security assessment. IET generation, transmission & distribution, 2012; 6(10), 1029-1035.

[17]. Zu, G., Xiao, J., & Sun, K. Mathematical base and deduction of security region for distribution systems with DER. IEEE Transactions on Smart Grid, 2018; 10(3), 2892-2903.

[18]. Xiao, J., Zu, G., Gong, X., & Li, F. Observation of security region boundary for smart distribution grid. IEEE Transactions on Smart Grid, 2015; 8(4), 1731-1738.

[19]. Xiao, J., Zu, G. Q., Gong, X. X., & Wang, C. S. Model and topological characteristics of power distribution system security region. Journal of Applied Mathematics, 2014. Available Online: https://www.hindawi.com/journals/jam/2014/327078/abs/

[20]. Zu, G., Xiao, J., & Sun, K. Distribution network reconfiguration comprehensively considering N− 1 security and network loss. IET Generation, Transmission & Distribution, 2018; 12(8), 1721-1728.

[21]. Yang, T., & Yu, Y. Static voltage security region-based coordinated voltage control in smart distribution grids. IEEE Transactions on Smart Grid, 2017; 9(6), 5494-5502.

[22]. Yang, T., & Yu, Y. Steady-State Security Region-Based Voltage/Var Optimization Considering Power Injection Uncertainties in Distribution Grids. IEEE Transactions on Smart Grid, 2018; 10(3), 2904-2911.

[23]. Wei, W., Liu, F., & Mei, S. Dispatchable region of the variable wind generation. IEEE Transactions on Power Systems, 2014; 30(5), 2755-2765.

[24]. Wang, B., Xiao, J., Zhou, J., Zhou, H., Liu, YL, & Zu, GQ. Dispatchable region of distributed generators and microgrids in distribution systems. Power System Technology, 2017; 41 (12), 363-370. (in Chinese)

[25]. Hu, J., Wang, P., & Wang, Y. Affine algorithm for solving dispatchable region of distributed generators with uncertainty in three-phase unbalanced distribution networks, Automation of Electric Power Systems, 2018; 42(10): 67-74 and 149. (in Chinese)

[26]. Cao, W., Wu, J., Jenkins, N., Wang, C., & Green, T. Operating principle of Soft Open Points for electrical distribution network operation. Applied Energy, 2016; 164, 245-257.

[27]. Farivar, M., & Low, S. H. Branch flow model: Relaxations and convexification—Part I. IEEE Transactions on Power Systems, 2013; 28(3), 2554-2564.

[28]. Xiao, J., Liu, S., Li, Z., & Li, F. Loadability formulation and calculation for interconnected distribution systems considering N-1 security. International Journal of Electrical Power & Energy Systems, 2016; 77, 70-76.

[29]. Xiao, J., Zhang, B., & Luo, F. Distribution Network Security Situation Awareness Method Based on Security Distance. IEEE Access, 2019; 7, 37855-37864.

[30]. Technical guidelines for distribution network. Q/GDW 10370-2016, China. (in Chinese).

[31]. Billinton, R., & Jonnavithula, S. A test system for teaching overall power system reliability assessment. IEEE transactions on Power Systems, 1996; 11(4), 1670-1676.